Selectivity and competition between the anodic evolution of oxygen and chlorine

Vos, J.G.

2

MEASUREMENT OF COMPETITION BETWEEN THE EVOLUTION OF OXYGEN AND CHLORINE USING RRDE VOLTAMETRY

Selectivity determination between chlorine evolution and oxygen evolution is not always straightforward, as most methods for measuring chlorine evolved are cumbersome and have slow response times. We therefore developed a new method to quickly measure that a Pt ring fixed at 0.95 V vs. RHE in a solution of pH 0.88 can selectively reduce the Cl_2 formed on the disk, which allows precise and flexible data acquisition. Using this method, we demonstrate that oxygen evolution and chlorine evolution on a glassy carbon supported IrO_x catalyst proceed independently, and that the selectivity towards chlorine evolution rapidly approaches 100% as $[Cl^-]$ increases from 0 to 100 mM. Our results suggest that on IrOx, oxygen evolution is not suppressed or influenced by the presence of Cl^- or by the chlorine evolution reaction taking place simultaneously on the surface.

THIS CHAPTER IS BASED ON THE FOLLOWING

PUBLICATION:

Vos, J. G.; Koper, M. T. M. Measurement of Competition between Oxygen Evolution and Chlorine Evolution Using Rotating Ring-Disk Electrode Voltammetry. J. Electroanal. Chem. 2018, 819 (October), 260–268.

2.1. Introduction

The OER and CER are strongly coupled reactions, and will proceed simultaneously on most catalysts. If we want to develop anodes selective for the OER in (acidic) brine solutions or further minimize efficiency losses in the electrolysis step of the chlor-alkali process, the selectivity must be optimized towards only a single reaction. For that, one will need to understand the competition between the OER and CER in more detail. A reliable and easy method for the determination of the selectivity between the OER and CER would be of great interest.

Previous research on the CER in aqueous media has generally been done in acidic solutions with very high Cl^- concentrations, often in the range of 3-5 M.[56,113,118–122] CER activity and Tafel slopes in such studies were derived from raw electrode current densities, with the assumption that all observed current could be ascribed to the CER and that the OER plays a negligible role. Although this assumption is reasonable for high Cl^- concentrations, a complete picture of the competition between the OER and CER in chloride-containing media cannot be drawn in this way.

An analytical method to measure Cl_2 and O_2 evolution separately, irrespective of chloride concentration, is Differential Electrochemical Mass Spectrometry (DEMS),[71,123–126] which directly probes Cl_2 vs. O_2 formation near the electrode surface and can provide highly accurate and quantitative results online.[29,70,127] However, DEMS suffers from inflexibility due to specific cell and electrode requirements, and relatively slow response times. Alternatively, a common method of selectivity determination is long-term bulk electrolysis, followed by titration of the working solution using diethyl-phenylenediamine salts (DPD) or iodometry, to determine the amount of Cl_2 formed.[29,73,128,129] This type of method, although accurate, is not suitable for generation of extended data sets and does not offer the online selectivity determination that DEMS does.

In this chapter, we explore a new method for measuring selectivity between the OER and CER in acidic chloride-containing media, based on conventional electrochemical methods. We develop and study the suitability of a rotating ring-disk electrode (RRDE) setup, which has been well established for faradaic efficiency (FE) measurements in benchmarking OER catalysts,[66,130,131] and for the detection of the formation of H_2O_2 during the oxygen reduction reaction (ORR) on model PEM fuel cell cathodes.[132–134] To the best of our knowledge, an RRDE approach for OER vs. CER selectivity measurements has not been previously reported. We used a Pt ring for Cl_2 detection during catalyst operation, as Pt was previously established as an effective catalyst for the chlorine reduction reaction (CRR), which is the opposite of the CER.[135] Other materials (such as Ru or Ir) may also be possible for Cl_2 detection,[136] but we have not pursued this in detail. As proof of concept, we explore the CER vs. OER behavior of IrO_x nanoparticles, as this material constitutes a stable and active acidic OER and CER catalyst.

2.2. Experimental

$KHSO_4$ (EMSURE), KCl (EMSURE), and $HClO_4$ (60%, EMSURE) were purchased from Merck. $Na_2IrCl_6 \cdot 6H_2O$ (99.9%, trace metals basis) and NaOH (30% solution, TraceSelect) were purchased from Sigma-Aldrich. All chemicals were used as received. The water used for cleaning glassware and preparing solutions was filtered and deionized using a Merck Millipore Milli-Q system (resistivity 18.2 MΩcm, TOC < 5 p.p.b.). Experiments were done in a home-made two-compartment borosilicate glass cell of 100 mL volume. IrO_x deposition experiments were done in a borosilicate glass vial of approximately 5 mL. Before the first-time use, all glassware was thoroughly cleared from organic contaminants by boiling in a 3:1 mixture of concentrated H_2SO_4 and HNO_3. When not in use, all glassware was stored in a 1 g/L solution of $KMnO_4$ in 0.5 M H_2SO_4. Before each experiment, glassware was thoroughly rinsed with water, and then submerged in a dilute solution of H_2SO_4 and H_2O_2 to remove all traces of $KMnO_4$ and MnO_2. The glassware was then rinsed three times with water, followed by triple boiling in Millipore water.

All experiments were carried out at room temperature (~20 °C). Hydrodynamic measurements were performed using an MSR rotator coupled to E6 ChangeDisk RRDE tips in a PEEK shroud (Pine Research Instrumentation). As counter electrode, a Pt mesh separated from the main solution by a glass frit was used. The reference electrode was a HydroFlex® reversible hydrogen electrode (Gaskatel). All potentials in this chapter are reported using the RHE scale. Using a Luggin capillary, the RHE reference was aligned to the center of the RRDE tip to minimize electrical cross-talk.[137,138] The liquid phase collection factor of the ring-disk system, N_l, was determined to be 0.245 in at least four separate experiments, where the GC disk was exchanged in between. The value was found using a conventional collection factor experiment on a freshly prepared blank GC electrode with a Pt ring, studying the reduction/re-oxidation of 10 mM $K_3Fe[CN]_6$ in 0.1 M KNO_3. 0.5 M $KHSO_4$ solutions were used for all CER activity experiments. pH values were 0.88 ± 0.05, as measured with a Lab 855 meter equipped with a glass electrode (SI Analytics). pH values were verified by measuring the potential of a calibrated Ag/AgCl reference electrode in the solutions. All working solutions were saturated with either O_2 or Ar (Linde, purity 6.0) before experiments. Mild gas bubbling through the solution was allowed during forced convection experiments, in all other cases gas was used to blanket the solution.

The electrochemical experiments were controlled with an IviumStat potentiostat (Ivium Technologies). For all experiments, the solution resistance was measured with electrochemical impedance spectroscopy, by observing the absolute impedance in the high frequency domain (100 KHz). Potentials were 85% corrected for these values during measurements. Before a CER activity experiment, the Pt ring was electropolished by cyclic voltammetry (CV) from -0.1 V to 1.7 V at 500 mV s^{-1} for 30 scans at a 1500 RPM rotation rate, after which the individual scans did not change. This step is vital to the removal of traces of alumina, as well as traces of IrO_x that tend to remain on the ring after being swept outward during IrO_x electroflocculation under rotation.[139] OER and CER experiments were done under hydrodynamic conditions at 1500 RPM by scanning the disk electrode in the range of 1.3 – 1.55 V at 10 mV s^{-1}. For quantitative analysis, the forward and backward sweeps were averaged to reduce

contributions from double layer charging and IrO_x pseudocapacitance. In between experiments, the IrO_x film was kept at 1.3 V. Ring currents were corrected for background currents and collection delay, which was approximately 200 ms at 1500 RPM. Before proceeding with OER and CER activity measurements, the IrO_x film was treated by performing 20 scans between 1.3 – 1.55 V, in absence of Cl^-. This was done to ensure stable and reproducible catalyst behavior during experiments.

IrO_x nanoparticles electroflocculated on glassy carbon were used as active OER/CER catalyst. The IrO_x/GC electrodes were prepared as described in sections 9.1.1 and 9.1.2. Al_2O_3 was used for GC polishing, followed by rinsing and 5 minutes sonication in acetone and water. A time duration of 600 s was used for the electroflocculation amperometry step.

For iodometry experiments, amperometry was performed for 60s at 1500 RPM in 16 mL of 0.5 M $KHSO_4$, in the presence of Cl^-, followed by titration of the bulk solution. Under identical conditions, amperometry was performed for 20s and the Pt ring was used to measure selectivity towards the CER. This selectivity was then applied to disk currents of the iodometry experiment to calculate the amount of Cl_2 that must have formed according to the RRDE method. In this way, both methods could be applied to a single experiment. The experiments were done in a glass vial without headspace, of approximately 16 mL volume. The vial was vertically elongated to minimize the contact area of the solution with air, and thus to prevent gaseous Cl_2 from escaping the acidic solution. All solutions were pretreated by briefly evolving chlorine and then purging the solution with Ar. Immediately after finishing an experiment, a large (~100x) excess of NaI was rapidly added to the solution to trap all Cl_2 as I_3^- and to minimize the equilibrium concentration of volatile I_2. The vial was then closed air-tight and the solution was allowed to equilibrate for approximately 1 minute. Iodometry was performed directly after. Reported values were the average of four titrations. For the sake of verification, RRDE experiments in the iodometry vial were compared to those in a standard glass RRDE cell of 100 mL volume. Although the absolute measured currents of the iodometry vial were slightly lower than the RRDE cell, the ratio i_R/i_D (the 'apparent chlorine collection factor', N_{Cl_2}) was found to be exactly the same, indicating proper transport of Cl_2 from the disk to the ring in the iodometry vial. This justifies the comparison of our RRDE method and iodometry. We attribute the lower CER currents in the small volume iodometric cell to distortion of the hydrodynamic flow field, leading to lowered Cl^- mass transport.

2.3. Results and discussion

2.3.1. Aspects of selectivity between the OER and CER

As discussed in section 1.3, the formation of hypochlorous acid or hypochlorite becomes thermodynamically favorable as the solution pH increases. These species might form directly from an electrochemical reaction (Eq. 1.7 and Eq. 1.8), or through solution hydrolysis of Cl_2 formed during the CER (Eq. 1.9 and Eq. 1.10). Contrary to chlorine, the reduction of ClO^- and HClO are sluggish reactions on Pt, which reach diffusion limited conditions only at overpotentials near $\eta = 1$ V.[140,141] As such, we do not expect it possible to quantify these species

by means of the RRDE, since the criterion of reaching diffusion limitations before the ORR (which has an onset of approximately 0.95 V on Pt) cannot be reached. The formation of ClO^-/HClO thus has to be kept minimal, and $Cl_2(g)$ is the desired chlorine species for reduction. We expect that the RRDE approach is limited to acidic environments (pH < 2), where the focus is on direct (kinetic) competition of the OER vs. CER, and where both products are gases dissolved in the working solution.

2.3.2. *Application of the RRDE to OER vs. CER selectivity measurements*

To demonstrate the application of our RRDE method to measure the CER, Figure 2.1 shows the forward and backward scan average of an IrO_x catalyst in the potential region of 1.3 – 1.55 V, in an acidic electrolyte in presence of 20 mM Cl^-. Figure A 9.2.1 in the Supporting information shows a typical characterization CV in the region 0 V - 1.4 V. In Figure 2.1, the disk current (black line) was measured until 1.55 V, leading to a competition between the OER and CER above ca. 1.48 V. The Pt ring (grey line) was fixed at E_R = 0.95 V and performs reduction of Cl_2 (CRR, see next section). The ring potential 0.95 V was chosen well in the diffusion-limited regime of the CRR near the edge of the ORR onset on Pt in a chloride-free solution. In this way, the ring allows very precise observation of the onset and the rate of the CER.

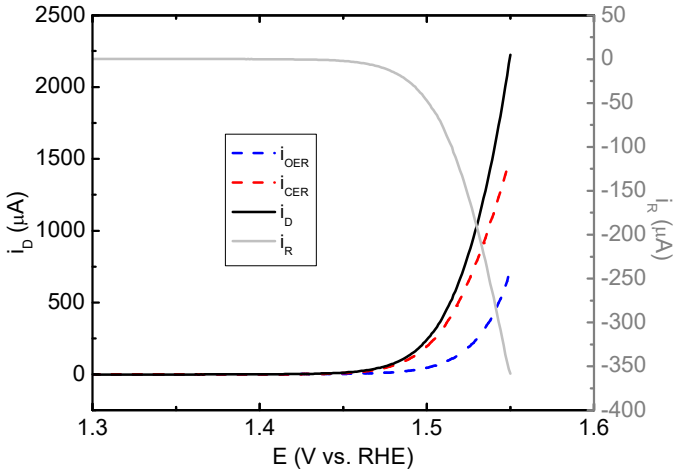

Figure 2.1: CV of IrO_x/GC in the OER + CER region in 0.5 M $KHSO_4$ + 20 mM KCl, scan rate 10 mV s^{-1}, rotation rate 1500 RPM. pH = 0.88, solution saturated with Ar. Ring potential was fixed at E_R = 0.95 V. The forward and backward scans of the disk were averaged, i_R was corrected for collection delay. i_{OER} and i_{CER} curves were calculated as described in the text.

To minimize capacitive charging contributions on the disk, a relatively slow scan rate of 10 mV/s was used, and values of forward and average scans were averaged. The magnitude of capacitive charging in the potential region of 1.3 V to approximately 1.4 V, where IrO_x experiences the onset of the Ir^{IV} to Ir^{V} transition, was approximately 10 µA. Such currents were usually less than 1% of the OER charge measured. Using the average of forward and backward scans eliminated most of this possible source of error, noting that our IrO_x showed no significant hysteresis in the 1.3 – 1.55 V potential range (see Figure A 9.2.1).

Since IrO_x is established as a stable acidic OER catalyst within the time frame of our experiments,[83] we assume that the measured disk current can be ascribed exclusively to either the OER or CER, after minimizing capacitive contributions. From the ring current, we can then separate the current contributions of the OER and CER on the disk. Since the chlorine reduction reaction taking place on the ring is simply the reverse of the CER, the current contribution originating from the CER, i_{CER}, will be:

$$i_{CER} = \left|\frac{i_R}{N_l}\right| \qquad \text{Eq. 2.1}$$

where i_R is the current measured on the ring, and N_l is the liquid phase collection factor ($N_l = 0.245$). The OER current contribution is simply the current remaining after subtracting CER activity:

$$i_{OER} = i_D - i_{CER} = i_D - \left|\frac{i_R}{N_l}\right| \qquad \text{Eq. 2.2}$$

where i_D is the total current measured on the disk. In Figure 2.1, i_{OER} and i_{CER} (blue and red dotted lines) were constructed by the above method. The OER onset is near 1.480 V, equivalent to an overpotential $\eta_{OER} \approx 0.25$ V, in agreement with previous studies.[142,143] The CER shows a much earlier onset of ~ 1.420 V, equivalent to a negligible overpotential at pH = 0.88.

At this point we must describe a significant caveat, namely, that there is always the risk of forming gas bubbles at high current densities. The problem is mainly related to high OER currents, which may rapidly lead to local supersaturation of poorly soluble O_2.[144–146] Gas bubbles may strongly persist on the electrode surface and hinder the transport of products to the ring,[147] compromising the quantitative nature of the experiment. This is a universal problem in the use of RRDE for gas forming reactions and makes OER FE experiments at high overpotentials extremely challenging. The solubility of Cl_2 around pH 1 is approximately 10^3 times higher than that of O_2,[148] making high CER currents less troublesome, although extreme CER current densities may additionally lead to formation of Cl_2 bubbles. Chapter 8 looks into this problem in much more detail.

2.3.3. Effect of chloride adsorption and PtO_x formation on chlorine detection with the Pt ring

To explore the behavior of the CRR (and the ORR) on the Pt ring in presence of Cl^-, we used the disk to generate a stepwise increasing Cl_2 flux, by fixing the disk potential in the range $1.420\ V < E_D < 1.480\ V$, where only the CER is expected to occur at pH = 0.88. We simultaneously recorded forward linear sweep voltammograms at 1500 RPM on the ring, using a slow scan rate of 5 mV s^{-1} to minimize transient charging current. The steady state disk currents and corresponding ring LSV profiles are shown in Figure 2.2. The working solution was saturated with O_2 to accurately monitor the ORR onset as function of $[Cl^-]$ and (locally) $[Cl_2]$. We assume that the increased concentration of O_2 does not majorly affect the CRR kinetics.

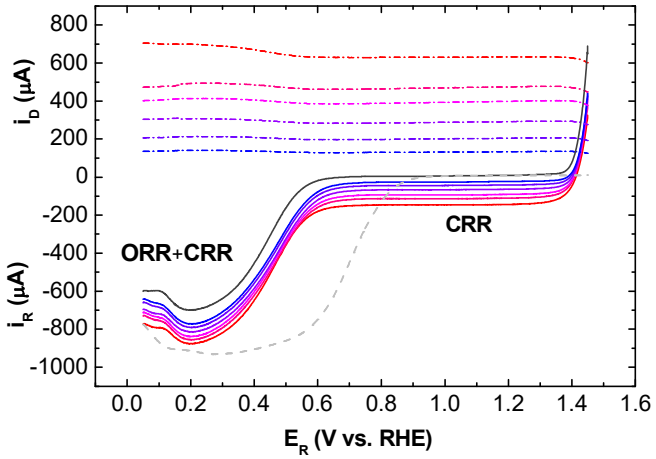

Figure 2.2: LSV of the Pt ring electrode, while keeping the IrO_x/GC disk electrode at constant potential in 0.5 M $KHSO_4$ + 100 mM KCl, scan rate 5 mV s^{-1}, rotation rate 1500 RPM. pH = 0.88, solution saturated with O_2. Dotted curves with positive values correspond to disk currents, remaining curves correspond to ring currents. The ring LSV sweeps were taken in the positive-going direction. Disk potentials were chosen in the region of exclusive chlorine evolution, with values increasing from the blue curve to the red curve, E_D = 1.449 V, 1.456 V, 1.462 V, 1.467 V, 1.470 V, and 1.475 V. Black curve shows ring response while disk is not connected. Grey dashed curve shows ring response while disk is not connected, in Cl^--free conditions.

In Figure 2.2, the ring first traverses a region of the superimposed ORR and CRR between 0.2 V $< E_R <$ 0.7 V. When comparing the ORR in chloride-free conditions (grey dashed curve), its onset potential in presence of 100 mM Cl^- is shifted 200 mV negatively, which prohibits the ORR from reaching diffusion limited current before the onset of hydrogen adsorption. Such a suppressing effect was previously observed by Schmidt *et al.*[149] even at [Cl^-] as low as 100 μM.

Following the ORR + CRR region, a region of constant negative current follows in the range of 0.7 V $< E_R <$ 1.3 V, which we ascribe to the CRR under diffusion limited conditions. At potentials higher than 1.3 V, the ring approaches $E^0_{Cl_2/Cl^-}$, and the onset of the CER on the ring can be observed. The experiments shown in Figure 2.2 were also performed for [Cl^-] = 150 mM and 200 mM.

It is reasonable to assume that the constant current in Figure 2.2 in the region of 0.7 V $< E_R <$ 1.3 V arises from the diffusion limited CRR. However, previous studies by Conway *et al.*[58,118] showed that chloride adsorption causes CER self-retardation on Pt for [Cl^-] ranges near 1 M by affecting the rate-limiting Tafel recombination step. To verify that the ring current response is completely diffusion controlled at E_R = 0.95 V, we propose a simple method: as long as only the CER occurs on the disk, a of plot i_R vs. i_D would yield a straight line, with the 'apparent chlorine collection factor' N_{Cl_2} as slope. If N_{Cl_2} approaches the liquid phase collection factor N_l, the ring reaction is indeed diffusion limited, and the measured CRR current is quantitative. Kinetic limitations of the CRR on the ring would manifest as $N_{Cl_2} < N_l$.

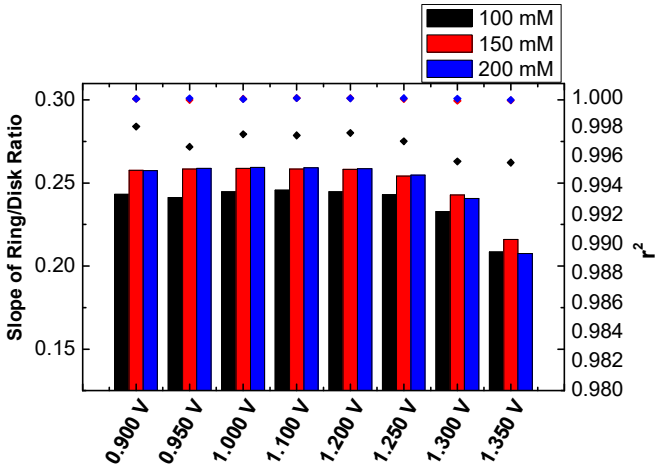

Figure 2.3: Apparent chlorine collection factors N_{Cl_2} (equivalent to slopes of ring/disk ratios) plotted as function of potential on the ring electrode, for $[Cl^-]$ = 100 mM (black), 150 mM (red) and 200 mM (blue). Diamonds (correspondingly coloured) indicate the determination coefficient r^2 of the found slopes. Data derived from Figure 2.2.

Using data from Figure 2.2, we plotted the i_R vs. i_D response at various ring potentials (see Figure A 9.2.2). We generally observed strong linearity between i_R and i_D, with determination coefficients r^2 approaching 1. Furthermore, as shown in Figure 2.3, N_{Cl_2} converges to a constant value of ~ 0.244 for $[Cl^-]$ = 100 mM, and ~ 0.258 for 150 mM and 200 mM, as E_R is lowered. Only for $E_R \geq 1.300$ V do we observe ring-disk ratios that significantly differ from these values. At these potentials, $E^0_{Cl_2/Cl^-}$ is approached ($\eta_{CER} < 100$ mV), and the CRR kinetics become kinetically limited. For $[Cl^-]$ = 150 mM and 200 mM, the value to which N_{Cl_2} converges is approximately 5% higher than N_l. We ascribe this discrepancy to electrochemical crosstalk,[137,138] which we could not eliminate experimentally despite intensive efforts (see also the slight downward slope in disk currents within 1.4-1.45 V, in Figure 2.2). Nonetheless, the most important point is that N_{Cl_2} reaches limiting values close or identical to N_l well before the ORR onset potential.

To explore the effect of pH on Cl_2 detection, and to corroborate the discussion in section 2.3.1 concerning pH-dependent Cl_2 disproportionation into hypochlorous acid, we have probed the apparent chlorine collection factor N_{Cl_2} in pH = 0.90 and pH = 2.91, using a forward linear sweep in a Pt-Pt RRDE setup. Figure A 9.2.3 in the Supporting information shows that N_{Cl_2} decreases from 0.242 at pH = 0.90 to 0.214 at pH = 2.91. We ascribe this 12% decrease in collection efficiency to the partial disproportionation of Cl_2 into HClO, a species which is undetectable by Pt at E = 0.95 V. Cl_2 detection is thus no longer quantitative at pH ~ 3, although it could still be used qualitatively, such as for mechanistic studies.

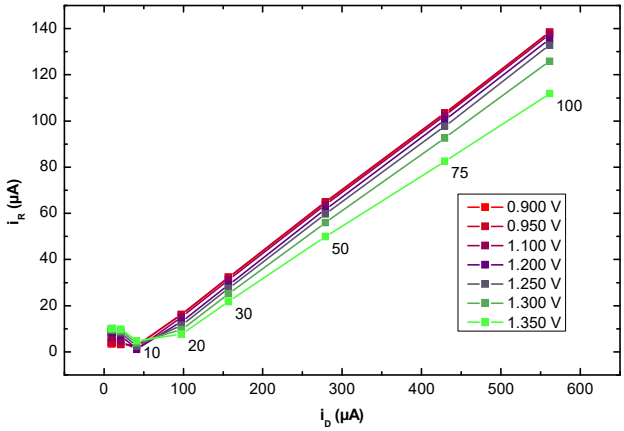

Figure 2.4: Behavior of i_R vs. i_D at various ring potentials. IrO_x/GC disk electrode fixed at 1.475 V, in 0.5 M $KHSO_4$ + $[Cl^-]$ increasing from 1 to 100 mM. Numeric labels next to data points show the concentration of chloride, in mM. Labels for $[Cl^-] < 10$ mM are not displayed.

Another factor that needs to be considered for the CRR on Pt is the presence of platinum oxide, which is known to be a sluggish CER/CRR catalyst in comparison with Pt.[58,108,135,136] In Figure 2.3, where $[Cl^-]$ is always 100 mM or higher, the formation of PtO_x can be assumed absent due to inhibition by Cl^- adsorption,[58] but lower $[Cl^-]$ would allow significant growth of oxides. To investigate the presence and effect of PtO_x on the CRR, we performed experiments as in Figure 2.2 and Figure 2.3, but instead, we fixed E_D = 1.475 V and studied the CRR on the Pt ring as function of $[Cl^-]$ increasing from 1 to 100 mM.

Like Figure A 9.2.2, Figure 2.4 displays slopes of i_R vs. i_D, together with the corresponding $[Cl^-]$ values. We note that an increase in $[Cl^-]$ will now have a twofold effect: a) it will increase CER current on the disk electrode, leading to higher Cl_2 flux to the ring and thus larger CRR currents, and b) it is expected to progressively inhibit PtO_x growth on the ring, affecting measured ring current profiles. Linearity between i_R vs. i_D is generally observed, except for data for which $[Cl^-] < 10$ mM. The corresponding LSV curves (see Figure A 9.2.4 in the Supporting information, inset) suggest significant PtO_x formation is taking place for measurements in the 1-10 mM range when comparing against the black curve taken in Cl^--free conditions. There is clear nonlinear behavior of increases in CRR current versus $[Cl^-]$. Only for $[Cl^-] > 10$ mM we observe the desired linearity. We explain these results as follows: for very low $[Cl^-]$, detrimental PtO_x formation occurs on the ring in the forward scan within the timescale of our experiments. For $[Cl^-] > 10$ mM, PtO_x growth becomes inhibited and the CRR may proceed on an oxide-free surface. For higher chloride concentrations, the i_R vs. i_D slopes show behavior identical to Figure 2.3, converging to $N_{Cl_2} \approx 0.247$ as E_R becomes lower.

To summarize our findings regarding the use of a Pt ring for chlorine detection: contrary to the ORR, the specific adsorption of chloride at Pt does not seem to have a detrimental effect on the CRR, at least not up to $[Cl^-] = 200$ mM. Somewhat ironically, Cl adsorption actually seems favorable for carrying out the CRR as it inhibits the formation of PtO_x, which *is* detrimental. Furthermore, in case of $[Cl^-] > 10$ mM, ring potentials of 1.250 V already seem

adequate to ensure that, at pH 0.88, the CRR proceeds diffusion limited. It is however recommended to keep the potential at the lowest possible limit, 0.95 V, to minimize growth and interference of PtO_x at lower chloride concentrations.

2.3.4. OER vs. CER selectivity as a function of E_D and [Cl⁻]

Based on the method described in section 2.3.2, we define the selectivity towards the CER (ε_{CER}) as the molar ratio of Cl_2 formed versus the total amount of Cl_2 and O_2 formed. This is equivalent to the ratio of CER current and combined OER and CER currents after normalizing them to the number of electrons in each reaction:

$$\varepsilon_{CER} = 1 - \varepsilon_{OER} = \frac{i_{CER}/2}{i_{CER}/2 + i_{OER}/4} \qquad \text{Eq. 2.3}$$

Typical results are displayed in Figure 2.5. We have plotted the data of three different disk potentials, namely a) 1.48 V, b) 1.52 V and c) 1.55 V. These potentials correspond to regimes where a) the CER is present and the OER is virtually absent, b) chlorine evolution is the major reaction but the OER takes place with a modest rate, c) both the CER and the OER take place.

From Figure 2.5 we can make several interesting conclusions. The CER activity is approximately linear with $[Cl^-]$ at all potentials, indicating a reaction order of one within the whole potential range. Only at very low $[Cl^-]$ we observe a slope smaller than one, likely due to PtO_x formation on the ring, as discussed in section 2.3.3. Furthermore, the OER rates show a constant value for a given E_D as function of $[Cl^-]$, and this trend persists in the entire measured potential range. Thus, the OER does not seem strongly affected by either the presence of Cl^- or the competing CER. Figure 2.5 suggests that the OER and CER proceed independently within the measured potential range. This implies that the OER and CER do not share the same active site on this catalyst, even though a scaling relationship between their activities has been suggested in previous literature.[55,72,76]

Extensive DFT calculations on model $RuO_2(110)$ surfaces have suggested that the OER and CER proceed on the same active site, namely, oxygen atoms (O_{ot}) bound to Ru atoms which are coordinatively unsaturated on the pristine model surface.[74,75] Although our results appear to exclude a model of two reactants competing for the same active site, it can be assumed that the amorphous, hydrous IrO_x catalyst in our study is far removed from the Ru single crystalline model surfaces used in the DFT studies, making a direct comparison difficult. Additionally, an independence of OER activity versus $[Cl^-]$ was previously found in DEMS studies on heterometal doped RuO_2 mixtures, indicating that such behavior is not unusual.[73,79]

As the chloride concentration increases, ε_{CER} appears to rise sharply. Near $[Cl^-] = 20$ mM, ε_{CER} generally exceeds 80%, and at 40 mM it exceeds 90%. When the chloride concentration increases to 100 mM, ε_{CER} converges to values above 95%. For comparison, Figure A 9.2.5 shows a similar ε_{CER} vs. $[Cl^-]$ plot for commercial RuO_2 (available from Sigma-Aldrich).

Interestingly, RuO_2 generally shows a higher selectivity towards the CER compared to the IrO_x catalyst, since ε_{CER} converges towards 100% CER more rapidly as $[Cl^-]$ increases.

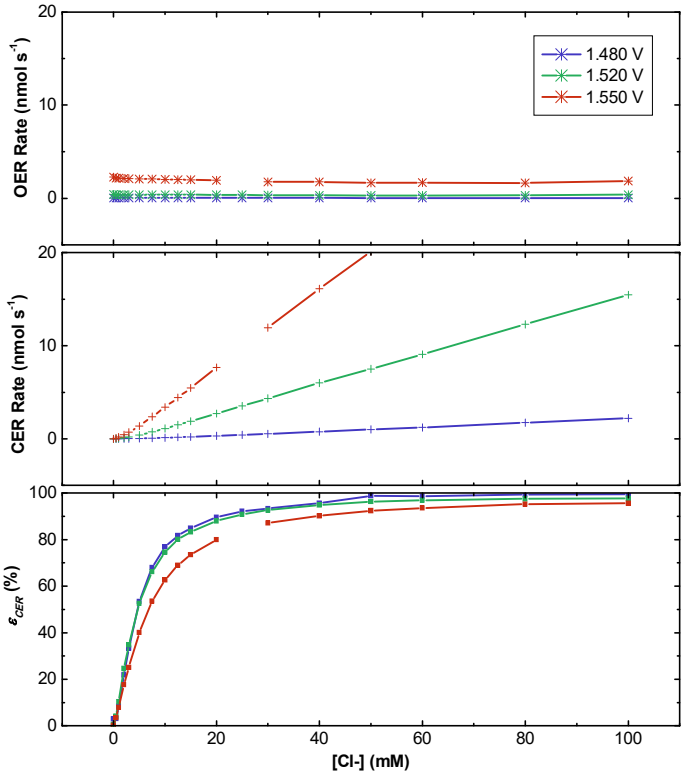

Figure 2.5: Plots of OER and CER reaction rates as function of $[Cl^-]$*, for three disk potentials:* $E_D = 1.480\ V$ *(blue lines),* $1.520\ V$ *(green lines), and* $1.550\ V$ *(red lines). Values were obtained from CVs identical to Figure 2.1, while varying* $[Cl^-]$*. Rates were obtained by dividing currents by nF, the number of electrons transferred and Faraday's constant.*

When the potential increases to 1.55 V, the CER starts becoming diffusion controlled, as indicated by increasingly higher Tafel slopes (not shown). Also, the CER selectivity starts to decrease due to diffusion limitations and increasing contributions of the competing OER. There is thus a range of low $[Cl^-]$ where significant (more than 10%) oxygen evolution is present regardless of potential, up to about $[Cl^-] = 40$ mM. Most importantly, higher potentials of catalyst operation will increasingly favor the OER. This trend is very similar to a previous DEMS study on OER vs. CER selectivity on pristine and doped IrO_x nanoparticulate catalysts.[150]

It needs to be stressed that that all measurements in this chapter were done in presence of 0.5 M HSO_4^-, which is known to adsorb on Pt.[151] To investigate the effect of anion adsorption on PtO_x formation and CER detection, ε_{CER} vs $[Cl^-]$ was measured in electrolytes of pH ~0.8 composed of 0.5 M $NaHSO_4$ and 0.5 M $NaClO_4$ (Figure A 9.2.6). A small but clear difference is apparent: although the two electrolytes show similar selectivities, ε_{CER} appears to lag behind in low $[Cl^-]$ regimes in presence of non-adsorbing ClO_4^-. We ascribe this to a greater degree of

PtO_x formation, which hinders Cl_2 detection and distorts the apparent selectivity. As discussed in section 2.3.3, the problem resolves itself as $[Cl^-]$ increases.

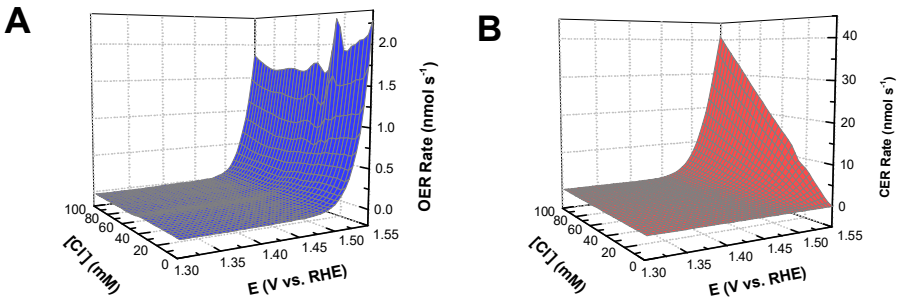

Figure 2.6: Plots of A) OER rates and B) CER rates as function of E_D and $[Cl^-]$, constructed from CVs identical to Figure 2.5, while varying $[Cl^-]$. Rates were obtained by dividing currents by nF, the number of electrons transferred and Faraday's constant.

Owing to the scanning nature of the experiments, we have sampled the complete potential range within 1.3 – 1.55 V. This allows the construction of 3-dimensional plots showing OER rates and CER rates as a function of E_D and $[Cl^-]$, as shown in Figure 2.6. We remark that 'dynamic' potential methods such as cyclic voltammetry may lead to different catalyst behavior than steady state measurements, especially concerning gas forming reactions.[82,152] In this chapter, we have only included cyclic voltammetry to serve as a proof of principle for the RRDE method, although steady-state amperometry experiments are also possible. Lastly, we stress that plots like Figure 2.5 and Figure 2.6 are only valid for stable catalysts. Side reactions and transient dissolution of the catalyst will distort the results. Caution is advised with the assumption that all remaining current is related to the OER.

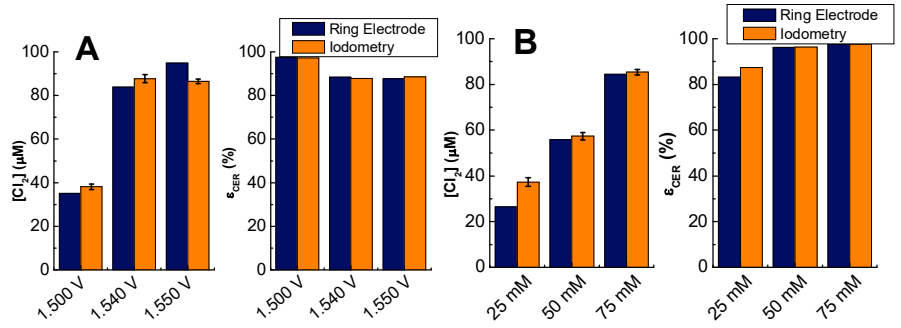

Figure 2.7: Cl_2 concentrations and corresponding ε_{CER} as determined by iodometry and the RRDE method, in 0.5 M $KHSO_4$. A: 50 mM KCl, as function of E_D. B: E_D = 1.53 V, as function of $[Cl^-]$. Error bars show 95% confidence intervals of the titration.

Finally, to confirm that the RRDE method yields trustworthy results, we employed iodometry to compare values of CER faradaic efficiency as determined by iodometric titration versus those determined by the RRDE method. Values of $[Cl_2]$ obtained versus E_D and $[Cl^-]$ are shown in Figure 2.7, and agree well with each other between the two techniques. Values of ε_{CER} versus E_D and $[Cl^-]$ correspond to those in Figure 2.5, but are approximately 3% lower.

As described in the experimental section, we ascribe this difference to a slight hindrance of Cl^- mass transport in the iodometry setup.

2.4. Conclusions

In this work, we described the application of an RRDE setup to measure rates of the chlorine evolution reaction in the context of selectivity between chlorine evolution and the evolution of oxygen in acidic aqueous media. We used a Pt ring to selectively reduce the Cl_2 formed on the disk by fixing the ring potential at 0.95 V vs. RHE in pH 0.88, which gives reliable diffusion limited chlorine reduction rates and allows precise and flexible data acquisition. Using this method, we demonstrated that the evolution of O_2 and Cl_2 on a glassy carbon supported IrO_x catalyst proceed independently, and that the selectivity towards chlorine evolution rapidly approaches 100% as the chloride concentration increases from 0 to 100 mM. Moreover, our results suggest that on IrO_x, oxygen evolution is not suppressed or influenced by the presence of Cl^- or by chloride oxidation taking place simultaneously on the surface.